Confirmation of Heavy-Component Rollup in Diffusion-Limited Fixed-Bed Adsorption

O. W. Haas, A. Kapoor, R. T. Yang
Department of Chemical Engineering
University of New York
Buffalo, NY 14260

Adsorptive separations are generally classified as either equilibrium- or kinetic-based depending on the importance of thermodynamic adsorption affinity relative to mass transfer limitations (Yang, 1987). When mass transfer resistances are small, local equilibrium between gas and solid may be assumed and adsorption affinity dominates. Kinetic separations assume that diffusional resistances are important resulting in the formation of concentration gradients within the adsorbent. The linear driving force (LDF) model makes the simplifying assumption that the intraparticle concentration profile is parabolic in shape (Liaw, 1979; Doong and Yang, 1986). Recently, Doong and Yang (1986) developed a bidispere pore diffusion model, in which the parabolic profile assumption has been employed to describe both macropore and micropore concentration profiles. The parabolic profile assumption is, however, valid only for long times after step changes, $D_i t/r_o^2 > 0.1$.

The kinetic separation of air (mainly for producing nitrogen) using molecular sieve carbon has been investigated by Jüngten (1977) and Hassan et al. (1986). Recently, the separation of nitrogen from air using 4A zeolite molecular sieve has also been described as a kinetic separation (Pan et al., 1988; Shin and Knaebel, 1987) because of the small micropore diameter of this adsorbent (4A) which approaches the molecular diameter of the adsorbates. Because of the small pore size, nitrogen has a significantly lower micropore diffusivity than does oxygen in these adsorbents. Kinetic separations attempt to take advantage of this disparity in diffusion rate to offset the higher equilibrium loading of nitrogen.

Concentration breakthrough curves in fixed-bed, multicomponent adsorption systems are used often to test the validity of adsorption models. A common characteristic of such breakthrough curves is the phenomenon of rollup wherein a lighter, weakly adsorbed component is displaced by a heavier, more strongly adsorbed component (Ruthven, 1984; Wankat, 1986; Yang, 1987). The lighter component is pushed ahead of and displaced by the advancing heavy component wavefront resulting in local concentrations which exceed the feed concentration for that component. Until recently, discussions of the phenomena have been described purely in terms of adsorption equilibria. The possibility of rollups caused by diffusivity differences was suggested only recently (Yang, 1987, p. 173). Kapoor and Yang (1987) modeled the phenomena considering micropore diffusion limitations. An interesting result of this work was the prediction of rollup for both the light and heavy components, the former being a result of equilibrium and the latter a result of diffusivity differences.

The objective of this work is to present breakthrough concentration profiles for the binary adsorption of oxygen (weak) and nitrogen (strong) on 4A zeolite molecular sieve. Of particular interest is the experimental confirmation of the strong component breakthrough behavior as predicted by Kapoor and Yang (1987).

Experimental Method

The adsorption column used in these experiments was made from a stainless steel pipe, 60 cm long and with an inner diameter of 4.1 cm. The column was packed with 0.16-cm pellets of 4A zeolite molecular sieve manufactured by Union Carbide Corporation. The sieve underwent an initial activation by dry helium purge at 300°C. A three-way valve at the top of the bed allowed the feed gas source to be switched between cylinder helium and dried plant air. The column pressure was maintained by means of regulators in the feed line and back-pressure regulator at the bottom of the bed. Flow was measured by means of a wet test meter placed in the exit line.

Gas samples were taken via syringe from a septum-equipped sample port located near the bed exit. The syringes could be locked so that a large number of samples could be taken for later analysis by gas chromatography (GC). A continuous record of effluent oxygen concentration was also provided by a paramagnetic oxygen analyzer (Servomex Model 0A137) and a re-

Correspondence concerning this paper should be addressed to R. T. Yang.

corder. Initial test conditions were set by adjusting valves and regulators while feeding dried line air to the bed. At this time, the oxygen analyzer was spanned and three samples of ambient air were taken by syringes for later analysis by GC. The feed gas was then switched to a helium purge (at feed pressure) for 15 to 20 minutes. The oxygen analyzer was then zeroed and three samples of the exit gas were analyzed by GC. After purging the bed with helium the feed gas was switched back to dried line air and the timer started. The effluent gas was sampled at short intervals by syringe while the oxygen concentration was recorded by the analyzer. Pressures, temperatures, and flow rates were recorded at the beginning and end of each run. The small amount of argon was not analyzed and was neglected in theoretical consideration.

Mathematical Models

Three models are presented for the breakthrough of O_2/N_2 mixture on 4A zeolite bed. The assumptions for the models are: ideal gas behavior, plug flow, isothermality (based on experimental observation of 4°C maximum temperature change due to adsorption) and negligible bed pressure drop.

The material balance equations for a binary mixture of N_2 (component 1) and O_2 (component 2) in the bed are:

$$\frac{\partial C_i}{\partial t} + \frac{\partial}{\partial z}(uC_i) + \frac{1-\epsilon}{\epsilon}\frac{\partial q_i}{\partial t} = 0; \quad i = 1, 2 \tag{1}$$

Substituting $C = P/RT$, $C_i = Py_i/RT$, $\partial P/\partial z = 0$ and assuming $\partial P/\partial t = 0$ we get

$$\frac{\partial y_i}{\partial t} = -u\frac{\partial y_i}{\partial z} + y_i\alpha_1 + \alpha_2; \quad i = 1 \tag{2}$$

and

$$\frac{\partial u}{\partial z} = -\alpha_1 \tag{3}$$

where

$$\alpha_1 = \frac{RT(1-\epsilon)}{P\epsilon}\frac{\partial}{\partial t}\left(\sum_{i=1}^{2} q_i\right) \tag{4}$$

and

$$\alpha_2 = \frac{-RT(1-\epsilon)}{P\epsilon}\frac{\partial q_i}{\partial t}; \quad i = 1 \tag{5}$$

Three different models were used to calculate $\partial q_i/\partial t$, which was then substituted in Eq. 1.

Case 1: equilibrium model

It is assumed that the mass transfer resistances are small, thus q_s' are replaced by q_s^*.

$$\frac{\partial q_i}{\partial t} = \frac{\partial q_i^*}{\partial t}; \quad i = 1, 2 \tag{6}$$

Case 2: linear drivigng force (LDF) model

It is assumed that mass transfer resistances can be expressed by the classic Glueckauf approximation.

$$\frac{\partial q_i}{\partial t} = \Omega(q_i^* - q_i); \quad i = 1, 2 \tag{7}$$

where

$$\Omega = \frac{15D_i}{r_o^2}$$

Case 3: pore diffusion model (PDM)

Because of crystal diffusion control for this system, the mass balance within an adsorbent particle is given by:

$$\frac{\partial q_i}{\partial t} = D_i\left(\frac{\partial^2 q_i}{\partial r^2} + \frac{2}{r_o}\frac{\partial q_i}{\partial r}\right) \tag{8}$$

The boundary conditions for the crystals are:

$$\left[\frac{\partial q_i}{\partial r}\right]_{r=0} = 0 \tag{9}$$

$$[q_i]_{r=r_o} = q_i^* \tag{10}$$

Equations 2–5 along with Eqs. 6–10 (depending on the model used) constitute the model. These model equations are solved with the following initial and boundary conditions for the bed.

Initial Conditions. Bed is assumed to be filled with helium at the adsorption pressure and temperature:

$$\begin{aligned} &\text{at } t = 0 \quad y_i = x_i = 0; \quad i = 1, 2 \\ &\qquad\qquad P = P_{\text{ads}} \\ &\qquad\qquad T = T_{\text{ads}} \end{aligned} \tag{11}$$

Boundary Conditions

$$\begin{aligned} &\text{at } z = 0 \text{ (feed end)} \quad u = u_{\text{feed}} \\ &\qquad\qquad y_i = y_{\text{feed}\,i}; \quad i = 1, 2 \end{aligned} \tag{12}$$

The equilibrium adsorption isotherms and diffusivities for O_2 and N_2 on 4A zeolite were measured in our laboratory. The equilibrium adsorption isotherms were fitted by Langmuir isotherm. The Langmuir and diffusion constants are in Table 1.

The model equations along with the initial and boundary conditions were solved by an explicit backward finite difference scheme. Typically, 60 distance steps and time step of 10^{-3}s were used for the computations. Langmuir isotherms were used to calculate q_i^*, then Eq. 6, 7 or 8, depending on the model used, was used to calculate $\partial q_i/\partial t$. Equations 4 and 5 were then used to calculate α_1 and α_2. Using these values of α_1 and α_2, u was calculated using Eq. 3. Finally, Eq. 2 was solved to give y_i at the next time step. The numerical scheme was stable for the range of conditions used in this study.

Results and Discussion

The concentrations of oxygen and nitrogen measured in the bed effluent were recorded as a function of time for each run. Data for a typical run are plotted in Figures 1 and 2. The nitrogen data points are from the GC analysis, while the oxygen data points were obtained from the continuous oxygen analyzer output chart. Sample lag time for the analyzer was corrected by matching its oxygen peak to that determined by the GC samples. Test conditions are also noted on Figure 1.

Table 1. Langmuir constants and crystal diffusivities in 4A zeolite at 298 K

Adsorbate	q_m^*, mol/g	B^*, 1/atm	D_i/r_o^2, 1/s
N_2	1.046×10^{-2}	14.493×10^{-3}	8.99×10^{-5}
O_2	1.561×10^{-2}	5.017×10^{-3}	8.51×10^{-3}

*Amount adsorbed, $q = q_m BP/(1 + BP)$

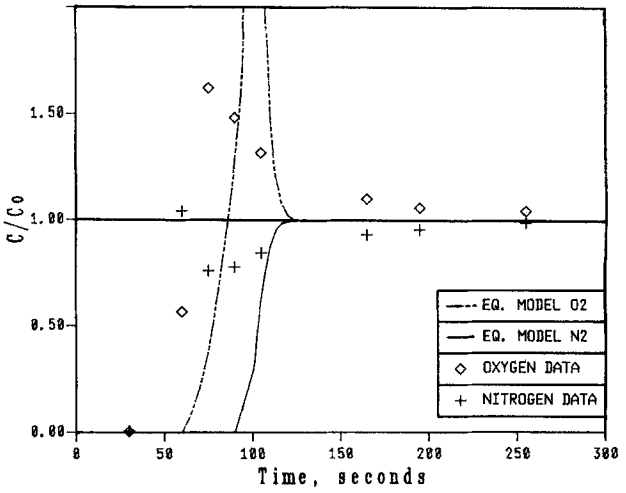

Figure 1. Breakthrough curves for O_2/N_2/4A zeolite system at 3 atm and 298 K with feed air at 3.8 L NTP/min.

Comparison between experimental result and equilibrium model prediction (r_o = 1.3 μm; ϵ = 0.4)

It is apparent from the plot that, under the experimental conditions, the breakthrough of oxygen and nitrogen occurs nearly simultaneously. In addition to the significant equilibrium-related rollup of the lighter (weaker adsorptive) oxygen component, there is a small, but readily discernible, diffusion-related nitrogen peak as well. This nitrogen peak was found to occur before the much larger oxygen rollup peak. Also illustrated in Figure 1 are the predictions of the three adsorption models discussed previously. The equilibrium model, which assumes no resistance to mass transfer, exhibits a relatively wide separation between the arrival of the two fronts and a single rollup for the weaker adsorptive. Since this model does not recognize differences in micropore diffusion rates, no heavy (strong) component rollup is predicted. However, the two kinetic models are successful in predicting both the closeness of the two breakthrough fronts and the presence of nitrogen (strong adsorptive) rollup. Of these two, the pore diffusion model (PDM) fits the data more closely having a lower nitrogen peak and higher oxygen peak than the linear driving force (LDF) model. This result is expected since the approximate LDF model has been found to deviate substantially from the exact solution at small values of diffusion dimensionless time, $D_i t/r_o^2$ (Do and Rice, 1986). This deviation is generally negative although significant positive deviations may also occur in the region of $D_i t/r_o^2 = 0.1$. Since the relative diffusivities, and hence the dimensionless times, for oxygen and nitrogen on 4A zeolite differ so widely, it is possible that the oxygen lies in the positive deviation region while the nitrogen is in the lower, negative deviation region.

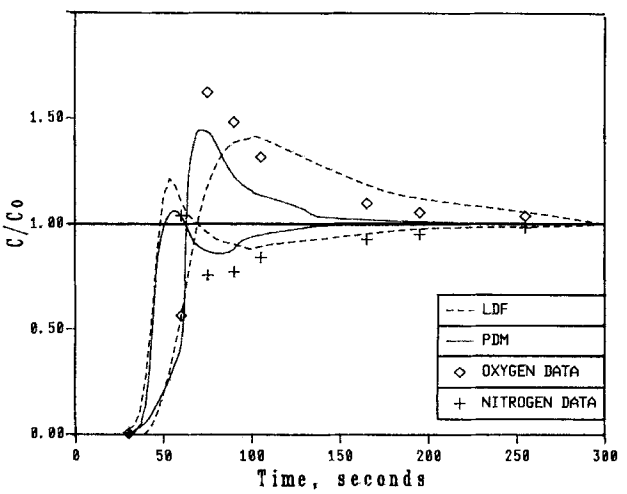

Figure 2. Breakthrough curves for O_2/N_2/4A zeolite system at 3 atm and 298 K with feed air at 3.8 L NTP/min.

Comparison between experimental results and predictions by kinetic models (r_o = 1.3 μm; ϵ = 0.4)

Acknowledgment

We acknowledge the support by the donors to the Petroleum Research Fund administered by the American Chemical Society.

Notation

C_i = concentration in gas phase, mol/cm^3
C_o = influent concentration, mol/cm^3
D_i = micropore diffusivity, cm^2/s
P = pressure in the bed, atm
q_i = adsorbate concentration, mol/cm^3
q_i^* = equilibrium adsorbate concentration, mol/cm^3
r = radial distance, cm
r_o = radius of crystals, cm
R = gas constant, atm · cm^3 · mol^{-1} · K^{-1}
t = time, s
T, = temperature, K
u = interstitial velocity, cm/s
x_i = mole fraction in adsorbed phase
y_i = mole fraction in gas phase
z = axial distance, cm
ϵ = fractional void in the bed
α_1, α_2 = defined by Eqs. 4 and 5
Ω = LDF constant defined by Eq. 7

Literature Cited

Do, D. D., and R. G. Rice, "Validity of the Parabolic Profile Assumption in Adsorption Studies," *AIChE J.*, **32**, 149 (1986).

Doong, S. J., and R. T. Yang, "Bidisperse Pore Diffusion Model for Multicomponent Pressure Swing Adsorption," *AIChE J.*, **32**, 397 (1986).

Hassan, M. M., D. M. Ruthven, and N. S. Raghavan, "Air Separation by Pressure Swing Adsorption on a Carbon Molecular Sieve," *Chem. Eng. Sci.*, **41**, 1333 (1986).

Jüntgen, H., "New Applications for Carbonaceous Adsorbents," *Carbon*, **15**, 273 (1977).

Kapoor, A., and R. T. Yang, "Roll-Up Phenomenon in Fixed Bed Multicomponent Adsorption Under Pore Diffusion Limitation," *AIChE J.*, **33**, 1215 (1987).

Liaw, C. H., J. S. P. Wang, R. A. Greenkorn, and K. C. Chao, "Kinetics of Fixed Bed Adsorption: A New Solution," *AIChE J.*, **25**, 376 (1979).

Pan, Z. J., R. T. Yang, and J. A. Ritter, "Kinetic Separation of Air by Pressure Swing Adsorption," *New Directions in Sorption Technology*, G. E. Keller, II and R. T. Yang, eds., Butterworth, Boston (1988).

Ruthven, D. M., *Principles of Adsorption and Adsorption Processes*, Wiley, New York (1984).

Shin, H-S, and K. S. Knaebel, "Pressure Swing Adsorption: A Theoretical Study of Diffusion Induced Separations," *AIChE J.*, **33**, 654 (1987).

Wankat, P. C., *Large Scale Adsorption and Chromatography*, Boca Raton, FL (1986).

Yang, R. T., *Gas Separation by Adsorption Processes*, Butterworth, Boston (1987).

Manuscript received Mar. 24, 1988, and revision received May 26, 1988.